A sensor fusion approach for drowsiness detection in wearable ultra-low-power systems

# A Sensor Fusion Approach for Drowsiness Detection in Wearable Ultra-Low-Power Systems

Victor Javier Kartsch[a,*], Simone Benatti[a], Pasquale Davide Schiavone[b], Davide Rossi[a], Luca Benini[a,b]

[a] *Micrel Lab - DEI, University of Bologna*
[b] *Integrated System Laboratory ETH, Zurich*

**Abstract**

Drowsiness detection mechanisms have been extensively studied in the last years since they are one of the prevalent causes of accidents within the mining, driving and industrial activities. Many research efforts were done to quantify the drowsiness levels using behavioral analyses based on camera eye tracking systems as well as by analyzing physiological features contained in EEG signals. Detection systems typically use specific drowsiness indicators from only one of these methods, leaving a risk of missed detection since not all the population presents same symptoms of drowsiness [1]. Thus, multi-feature systems are preferable even though most of the current State-of-the-Art (SoA) solutions are based on power-hungry platforms and they have meager chance to be used in embedded wearable applications with long battery lifetime. This work presents a drowsiness detection scheme fusing behavioral information coming from user motion through an IMU sensor and physiological information coming from brain activity through a single EEG electrode. The solution is implemented and tested on a low power programmable platform based on an ARM Cortex-M4 microcontroller, resulting in a wearable device capable to detect 5 different levels of drowsiness with an average accuracy of 95.2% and a battery life of 6 hours, using a 200mAh battery. We also study the energy optimization achievable by accelerating the sensor fusion-based drowsiness detector on a parallel ultra-low power (PULP) platform. Results show that the use of PULP as efficient processing platform provides an energy improvement of 63x with respect to a solution based on a commercial microcontroller. This may extend the battery life of the complete system up to 46 hours with a 7x improvement, paving the way for a completely wearable, always-on system.

*Keywords:*
Drowsiness Detection, Fatigue monitoring, EEG, Sensor Fusion, Wearable.

## 1. Introduction

Safety is a major challenge in transportation and automotive industries. According to Caterpillar, the world's largest manufacturer of construction and mining, fatigue is one of the most prevalent causes of earth-moving equipment accidents within the mining industry (large vehicles such as bulldozers and excavators) [2]. The shifts of the workers can often be 12-hours long, which increases the risk of "micro-sleeps" when suffering from fatigue, compromising the safety of the operations. This also applies for public transportation (buses, trains, planes, etc.). The USA National Highway Traffic Safety Administration (NHTSA) estimates that there are annually about 100,000 crashes in USA caused by fatigue, resulting in more than 1500 fatalities and 71,000 injuries [3]. In Europe, more than 20% of the car accidents are caused by this condition [4]. Thus, driver fatigue assessment remains a big challenge to meet the demands of future intelligent transportation systems [5].

During the last years, technology enhancement has enabled several new approaches for addressing fatigue monitoring and drowsiness detection. The automotive industry is currently exploring solutions based on in-vehicle sensors to monitor and prevent dangerous situations. For instance, lane detector systems [6] or semi-autonomous drive supports [7] have been proposed. Other systems can provide an indirect indication of the driver's level of fatigue by scanning the driving profile (acceleration, braking, etc.) and measuring the travel

*Corresponding Author
*Email addresses:* victorjavier.kartsch@unibo.it (Victor Javier Kartsch), simone.benatti@unibo.it (Simone Benatti), pschiavo@iis.ee.ethz.ch (Pasquale Davide Schiavone), davide.rossi@unibo.it (Davide Rossi), luca.benini@unibo.it, lbenini@iis.ee.ethz.ch (Luca Benini)

time.

Other approaches focus on the physical behavior of the driver to determine drowsiness. By using on-board cameras, eye and face tracking systems aim to monitor drivers eye parameters as PERCLOS (percent of time with eyelid closed at least 80%, measured in a minute) [8], eye blink ratio, blink duration, changes in driver's head inclination and yawing occurrence.

The aforementioned indirect methods are unobtrusive and can be useful in situations where users are forgetful. Nevertheless, they have to be embedded in the cockpits of the vehicles, and the high computational costs, complex hardware requirements and specific angle and illumination conditions (in case of camera systems) drastically limit the potential for portability.

On-board Inertial Measurement Units (IMUs) are also currently studied to determine behavioral drowsiness parameters, for example, some of those are deployed to track steering wheels movements [9]. Recently, similar devices were installed on helmets to evaluate head gesture providing alarms when drowsiness-related movements are detected [10]. These features, purely *behavioural*, represent an intuitive way to detect the drowsiness of a driver. However, since many of these movements generally occur also during normal working activities, the approach is subject to a high ratio of false positives [11].

The monitoring of physiological parameters has been extensively studied since biomedical signals are useful indicators of fatigue and drowsiness [12, 13, 14]. Indeed, heart rate, skin electric potential and brain activity evidence detectable changes in presence of drowsiness [15]. More specifically, some cars incorporate electrodes on the seat belts or on the steering wheels [16] to measure ECG (Electrocardiogram). Regrettably, this approach does not show promising results since it is prone to errors due to the lack of reliability of electrodes contact (e.g. gloves, heavy clothes, moving artifact, etc.) and due to the variability of the heart rate caused by other factors different than drowsiness [17, 18].

The analysis of EEG (Electroencephalography) signals is currently the most commonly used method to detect drowsiness. These signals result from the superposition of the individual contribution of the neuronal activity. EEG signals are mostly the result of the cortical activity, which corresponds to the external layer of the brain. Electrodes located on the head (partially or totally covering the scalp) extract the potential variations. Depending on the frequency bands, the signals can be classified as Delta waves (1-4$Hz$), Theta waves (4-8$Hz$), Alpha waves (8-13$Hz$), Beta waves (13-30$Hz$) or Gamma waves (30-50$Hz$). It has been demonstrated that the variation of the brain rhythms on the alpha waves band indicates a drowsy state [19]. However, the brain activity is highly subject-dependent and heavily affected by environmental noise. Moreover, alpha waves are not present in 10% of the world population [1, 20]. To increase the reliability of the detection, some systems integrating different sensors have been developed. These approaches are based on sensor fusion techniques combining different physiological parameters, either at system level [14, 21] or at chip level [22, 23].

This work presents a heterogeneous approach that merges behavioural and physiological monitoring exploiting sensor fusion techniques to detect drowsiness with a single-channel EEG and an IMU, leading to a minimally intrusive embedded device based on a low-power processor. By exploiting heterogeneous sensor fusion techniques the proposed system detects 5 drowsiness levels. Extracting features from alpha waves activity and from user movements, the proposed approach achieves a reliable detection among the test subjects.

Furthermore, the proposed solution is suitable for Body Area Network scenarios [24], since the Printed Circuit Board (PCB) designed for the application has a small form factor (9x4.5cm) and integrates all the components (i.e. a microcontoller, analog-to-digital converter (ADC), accelerometer, BT module, voltage converters and regulators) required for a real-time embedded drowsiness detection and low-power wireless transmission.

The proposed system, based on a commercial STM32 microcontroller, was tested on 10 subjects to evaluate the drowsiness level detection, achieving an average accuracy of 95.2% with a power consumption of the whole system of 109.93mW leading to a battery life of 6 hours using a 200mAh battery. Finally, a step further in energy efficiency is taken by implementing the drowsiness detection computations on a Parallel Ultra-Low Power (PULP) processor [25, 26] that combines a multi-core architecture with near-threshold operating voltage. Our optimized algorithm achieves almost ideal parallel speedup, fully unlocking the energy efficiency boost provided by low-voltage, low frequency parallel operation as opposed to faster sequential operation at higher operating voltage. The exploitation of PULP as processing platform drastically extends the battery lifetime to 46 hours, leading to an improvement of 7x with respect to the MCU-based solution, paving the way for a completely wearable, always-on system solution.

## 2. Related Work

Detection of driver's drowsiness is an active research field in both industrial and transportation areas. To increase safety and reduce the number of accidents, several automotive companies, universities, research centers, and governments are contributing to the development of Advanced Driver Assistance Systems (ADAS) aiming the analysis of different technologies and techniques to reduce the risk of accidents caused by drowsiness [2, 5].

Commonly, commercial vehicles identify safety risks by analyzing the driver's behavior, which includes the monitoring of the vehicles position with respect to the lane markings [27] and the steering wheel movements [28]. Although these systems trigger alarms when a dangerous driving situation is detected (e.g. when the vehicle goes out of the tracks), they are not able to alert the driver in advance on the occurrence of dangerous conditions, such as reduced attention caused by a high level of fatigue.

A more reliable approach is adopted in systems that measure physical behaviours (PERCLOS, Blink Frequency, Nodding and Yawing occurrences) to detect the level of fatigue. For example, the work presented by Flores et. al. [29] relies on a digital camera to compute the drivers eyes state and eyes blinking frequency, head movement and sagging body posture. Since this method is based on computer vision techniques, it results to be a challenging task due to the variability of environmental factors such as illumination conditions. Therefore, the addition of NIR (Near Infra Red) illumination and stereo vision is a common practice to operate in nocturnal conditions [30, 31]. Both implementations locate the position of the eye using image differences based on the *bright pupil effect*. On top of this, the blind eyelid frequency and eye gaze are computed to build drowsiness indices such as PERCLOS and AECS (Average Eye Closure Speed) [2]. The common drawback of the solutions based on computer vision is the need for high-performance computing systems to continuously process the huge stream of data generated by the cameras, such as small servers on the vehicles trunk. Moreover, two different kind of sensors are always required to deal with different lighting conditions and the line of sight has to be granted for a reliable recognition of the drowsiness indicators.

To overcome these issues, and to provide a more direct approach in the detection of drowsy driving situations, the new trend of research is to directly measure biometric signals such as EEG, EOG (Electrooculography), ECG, PPG (Photoplethysmogram), and eventually fusing data from multiple sensors [32, 33] to improve the robustness of the approach [34, 35, 36].

Among them, the system proposed by Lee et.al. [37], relies on sensor fusion algorithms to detect the drivers fatigue level using ECG, heart rate variability, blood pressure and PPG signals collected from an indoor driving simulation and processed by a smartphone. Reyes et. al. [38], proposed the integration of body area sensors and vehicular ad-hoc networks for traffic safety using a wireless physiological signal-acquisition module which collects and pre-process EEG signals to later send them to a small on-board PC for elaboration. Sun et. al. [39] demonstrates that ECG, EEG and eye blinking can be measured and exploited in the context of drowsiness detection in car environments. The experiments, conducted on a high fidelity driving simulator, show that the system is able to detect the ECG/EEG signals through clothes without skin contact. The drowsiness-estimation system proposed by Lin et. al. [40] is based on electroencephalogram (EEG) and combines independent component analysis (ICA), power-spectrum analysis, correlation evaluations and linear regression model to estimate a drivers cognitive state when the subject is in a virtual reality (VR)-based dynamic simulator. In Shuyan et. al. [41], eyelid parameters are extracted from the EOG data, collected in a simulated driving experiment to detect successfully the drowsiness of the drivers using Support Vector Machine (SVM). The driver fatigue recognition model of [40] is based on a dynamic Bayesian network. Multiple features, such as contextual (sleep quality) and physiological (ECG, EEG and eye movements) were evaluated, showing that the EEG and ECG signals contribute significantly to fatigue detection [23]. The aforementioned approaches are based on computationally intensive algorithms and require cumbersome setup and high-end computing platforms. On the other hand, the design of a minimally intrusive and low-power system is a desirable solution for better portability and longer battery lifetime.

Thanks to the lower computational effort required by the extraction of the physiological signals w.r.t. computer vision, some attempts have been made so far to use low-power microcontrollers as computing platforms, allowing to embed the whole system into wearable components. The wearable system proposed by Lin et. al. [42] is suitable for car applications and it includes a physiological signal-acquisition module and an embedded signal-processing module designed for real-time drowsiness detection. However, the signal processing module is still based on a power-hungry DSP processor (750mW) hence not suitable for autonomous long term monitoring. Similarly, [43] presents a system using

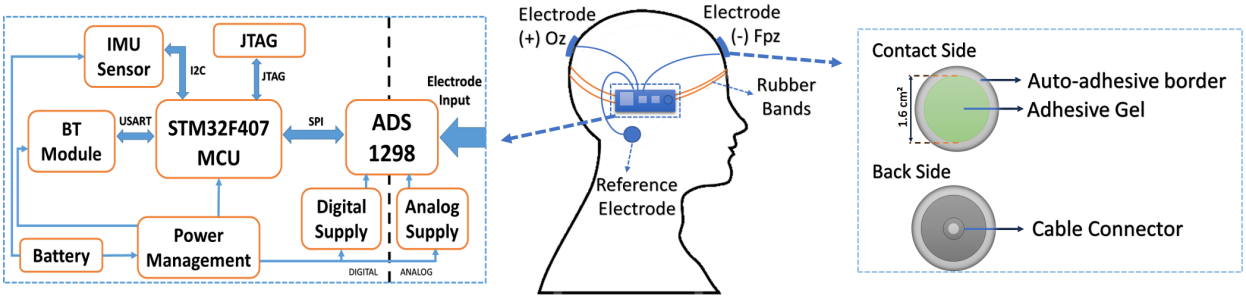


Figure 1: Block diagram of the board. The board is secured on the head using rubber bands. Auto adhesive circular gel-based electrodes are used to transmit the signals from the head to the ADC.

EEG and NIRS (NIR Spectroscopy), where the implementation is totally embedded, and the signal processing and the predictions are performed on the same system on chip (SoC), achieving an autonomy of 5 hours.

The Smart Safety Helmet, proposed in [10] consists of a low cost embedded system, exploiting an IMU and dry EEG electrodes connected to a 16-bit PIC microcontroller. A vibrotactile motor is integrated into the helmet to alert the operator when a computed risk level (i.e., fatigue, high stress or error) reaches a threshold. Once the risk level of accident surpasses the threshold, a notification is sent to a connected machine to stop the current work or process. The system is fully implemented and tested on 3 subjects. The activity recognition of torso and head movements is made by the IMU while the EEG alpha waves signal indicates the level of fatigue. This work exploits a sensor fusion algorithm based on IMU and EEG sensors integrated on a single wearable board, able to provide 5 levels of alarm, covering a wide variety of drowsiness-related symptoms. From the EEG sensors, three parameters are extracted. The first consists of the blink duration, since it increases when drowsiness is appearing and it is also related to micro-sleeps [44, 45, 46]. The second parameter counts the duration of alpha waves bursts since it is related to drowsiness [19]. The third, also related to the presence of alpha waves, detects the complete closure of the eyes [47] by considering the constant presence of alpha waves for a given time. From the IMU sensor, nodding, normal movement and no movement of the user are detected by evaluating the acceleration measured by the sensor. These behavioral and physiological indicators are combined on a fusion algorithm to provide 5 drowsiness related alarms, significantly improving the detection accuracy with respect to the state of the art, while performing all the processing and classification on a deeply embedded platform.

Furthermore, our detection algorithm have been implemented on a near-threshold parallel platform, providing a significant boost in energy efficiency with respect to traditional MCUs. This approach extends the battery-life of the system to 46 hours, significantly improving the battery-life of the proposed system with respect to the state of the art solutions, and paving the way to a wearable long-term monitoring platform.

## 3. System Architecture

Fig. 1 shows a high-level diagram of the proposed system. This section introduces the feature extraction methods and the architecture of the proposed drowsiness detection system, including the hardware platform, the detection algorithm and the sensor fusion approach adopted. The sensing subsystem of the platform relies on an ADC designed for EEG acquisition and on an IMU. These devices are connected via SPI and I2C, respectively, to a commercial ARM Cortex M4 microcontroller used to acquire the data and to perform the real-time detection. The on-board Bluetooth module can transmit the output of the detection, the EEG signal, or intermediate waves and information to a smartphone, tablet, or PC which can be used for debugging purposes, to visualize the output of the drowsiness detection, or most commonly just to notify to the user the different levels of alarm.

### *3.1. Feature extraction*

The evaluation of the behavioral and physiological parameters of the user is performed extracting the relevant features from the input signals. In this section, we introduce the methods used, separating them according to the type of signal. The combination of the processed features provides the different levels of alarm.

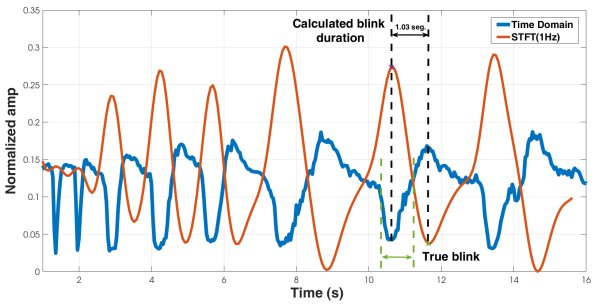


Figure 2: Blinks in time and frequency domain. The blue line represents the original EEG signal contaminated with the eye-blink artifacts (depressions of the signal) while the red line represents the energy values of the 1 Hz signals over time, extracted using the STFT.

### *3.1.1. EEG signals*

The EEG signal is extracted from the brain cells electrical activity and corresponds to the superposition of the cell membrane depolarizations [48]. EEG is acquired non-invasively with conductive electrodes placed on the scalp and connected to an instrumentation amplifier or to an ADC. The EEG signal amplitude ranges from 5 to 200$\mu$V. The low-pass effect and the spatial integration caused by the skull make the EEG acquisition highly prone to electrical noise, even though this signal, by virtue of its high temporal resolution (<1ms), is widely used in neurological analysis and in BMI systems. In this work, two features are extracted from EEG signals, described in the following.

*3.1.1.1. Blink Duration.* According to [44, 45, 46] the blink duration provides a clear indication of drowsiness since is associated to micro-sleeps events. Our implementation measures this parameter using the electrode configuration reported in Fig. 1, that allows the extraction of the blink duration from EEG signals avoiding the use of an extra EOG channel.

The blink duration is extracted by calculating the Short-Time Fast Fourier Transform (STFT) over 512 samples (1.024 seconds) with sliding windows of 32 samples (64 ms) for a frequency of 1Hz. Fig. 2 shows the energy of the STFT 1Hz during a series of blinks and the corresponding EEG signal in the time domain. For each blink, the presence of a high and low peak is evident and it is noticeable that longer blinks result to a higher amplitude in the frequency domain.

To remove artifacts such as eye movements, saccades, etc., the amplitude difference is compared to a threshold before being classified as a regular-long blink. The threshold is obtained empirically by acquiring amplitude differences from 3 test subjects, asked to blink the eyes at different frequencies and to move the eyeballs while keeping the eyes open, to generate artifacts. Hence, the normalized max-min difference of the STFT 1Hz energy and the average time of three different trials of Short Blink (SB), Middle Blink (MB) and Long Blink (LB) are calculated to extract the threshold. Results of this method are summarized in Table 1.

The accuracy is calculated comparing measured values against the definition of blink duration for EOG reported in [49], where the blink duration is estimated by finding the half-amplitude of the upswing and downswing of each blink and computing the time elapsed between the two.

Table 1: Normalized peak-to-peak difference for different blinks and detection accuracy. The accuracy was evaluated comparing the estimated values with the values obtained using the definition of blink given by [49].

| **Trial No.** | **SB** | **MB** | **LB** | NB | **Acc. %** |
|---|---|---|---|---|---|
| Trial 1 | 0.03 | 0.168 | 0.308 | 0.01 | 92 |
| Trial 2 | 0.03 | 0.168 | 0.290 | 0.009 | 93 |
| Trial 3 | 0.03 | 0.167 | 0.302 | 0.01 | 87 |
| Avg. time | 0.367ms | 0.61ms | 1.174ms | - | - |

*3.1.1.2. Alpha waves (AW) detection.* Alpha waves have been shown as a good indicator of fatigue, since the variation of the brain rhythms in this band indicates drowsiness. Two methods, based on threshold detection, have been evaluated to detect alpha waves bursts.

In the first method, the EEG signal is band-filtered to extract the alpha rhythms. We apply a 128-taps Finite Impulse Response (FIR) filter in the 7.5-13 Hz band. Therefore, the root-mean-square (RMS) is calculated over a sliding window of 250 samples with 125-samples overlap, to extract the signal envelope. Finally, the presence of alpha waves is detected only when the RMS envelope is above a given threshold. In the second method (PSD-method), we analyze the signal in the frequency domain. The STFT is calculated over 512 samples (1.024 seconds) with sliding windows of 32 samples (64 ms). Here, the power spectrum is calculated on the frequencies of interest (7.5-13 Hz) and the maximum value within this band is selected for each time step (64ms). Alpha rhythms are detected when the PSD value is above a given threshold.

In both cases, the thresholds were found experimentally, with a test on 3 subjects that were requested to open/close their eyes for a given time. The values are reported in Table 2, where the two methods are also compared in terms of classification accuracy. It is pos-

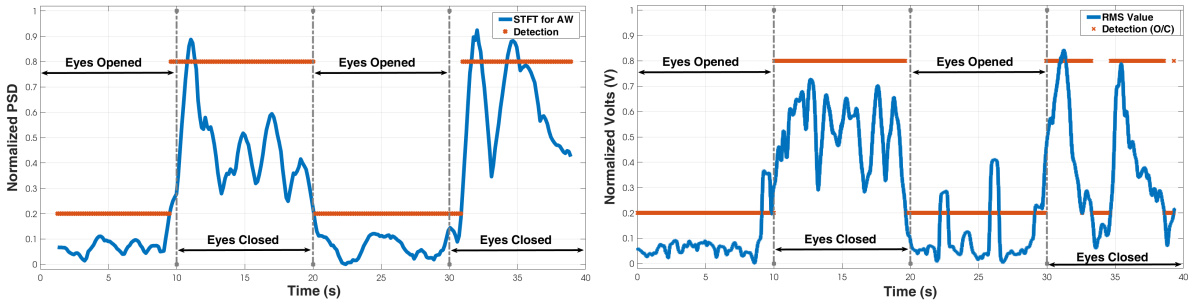


(a) (b)

Figure 3: Testing of the PSD and RMS methods. In both figures, a 40 seconds duration test is represented, the 10-20 and 30-40 second intervals correspond to the signal outputs where the test subject have the eyes closed. The reminding time intervals correspond to eyes opened. The red lines show the output of the prediction algorithm, where the lower lines represent eyes-opened detection and the higher lines represent the eyes closed detection. In (a), the blue line shows the maximum energy value among the the frequencies of the alpha waves band over time, extracted using the STFT. In (b), this line represents RMS envelope of the filtered original signal (band-pass filtered at 7.5-13 Hz to keep the alpha waves only).

sible to note that the second method based on the PSD reaches higher classification accuracy, therefore it has been selected for the final implementation (using the same thresholds for consecutive test subjects). Figures 3(a) and 3(b) show a 40 seconds example where the two methods try to classify the blink by checking if eyes are open or closed. From Fig. 3(a) it is noticeable that the RMS based method gives worse classification result than the PSD based one. Moreover, using frequency domain features at this level does not add any complexity to the detection algorithm since the STFT is already calculated in the blink duration estimation.

### *3.1.2. IMU signals.*

IMU sensors provide information about user gestures [52, 53]. The nod gesture is an important indication of sudden sleep and it was used in previous investigations [54, 55, 56]. Detecting such gesture is done via the RMS of derivative of the accelerometer signal on the three dimensions of 32 samples with sliding windows of 1 sample. The RMS calculation smooths the derivative signal to detect three activities: sudden tilt (ST), normal movement (NM) and no movement (NOM). Two thresholds are compared to the RMS value to assign one of the three activity states. If the RMS is greater than the higher threshold, the ST state is asserted. If the RMS is in between the two thresholds, the NM state is asserted. If the RMS is below the lower threshold, the NOM state is asserted. Fig. 4 shows an example of activity recognition where it is possible to see three peaks of the RMS value, which indicate a sudden tilt movement. Raw data was extracted from 3 test subjects wearing the device and later analyzed on MATLAB to find the optimal threshold values. The approach is tested by collecting data of the three different activities and evaluating the accuracy of the RMS decision tree. The accuracy of the classifier for the three different classes is reported in Table 3. After this evaluation, the threshold values were kept constant for the consecutive test with other test subjects.

Table 2: Comparison of the RMS and PSD method for alpha waves detection using optimal threshold. The metrics used here were selected considering their common use in other investigations [50][51]. The values were obtained after classifying eyes opened/closed events for the respective methods and optimal thresholds. Details of the experimentation are indicated in Figure 3(a) and 3(b) respectively.

| Method | Threshold | Sensitivity | Specificity | Accuracy |
|---|---|---|---|---|
| RMS | 0.4 | 0.882 | 0.934 | 0.908 |
| PSD | 0.2 | 0.900 | 0.997 | 0.949 |

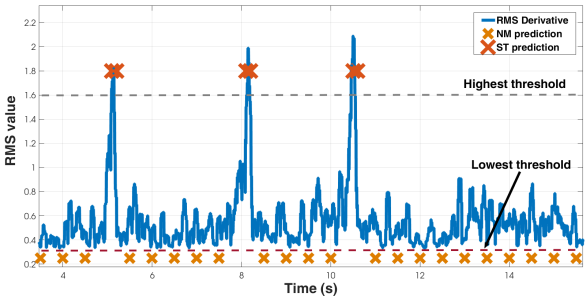


Figure 4: Detection of the activities using G-force and its derivative. Here, the sudden tilt and normal movement are correctly detected by the gesture classifier.

### 3.2. System Level Design

The block diagram of the proposed system is presented in Fig. 1. The EEG signals are acquired by the Texas Instrument ADS1298 low power ADC which is specifically designed for the acquisition of biopotentials like ECG, EMG and EEG [57].

The ADC has 8 differential channels with a resolution of 24 bits and its power consumption is 0.75 mW per channel in typical conditions. The sampling rate ranges from 250 Hz to 32 kHz. The proposed system uses only one differential channel at 500 Hz with two circular gel-based electrodes featuring a surface contact of 2 $cm^2$.

The InvenSense MPU-9150 Motion Processing Unit (MPU) has been used to capture the user motion. The MPU is a 9-axis motion tracking device which combines a 3-axis MEMS gyroscope, a 3-axis MEMS accelerometer, 3-axis MEMS magnetometer and a Digital Motion Processor hardware accelerator engine [58]. It has 16-bits resolution for each gyroscope and accelerometer axis and 13-bits resolution for the magnetometer.

The outputs of the EEG sensor and the MPU are transmitted to a microcontroller via SPI and I2C, respectively.

The STMicroelectronics STM32F407 microcontroller [59] is based on an ARM Cortex-M4 core with floating point unit, equipped with 192 kB of SRAM and 1 MB of non volatile Flash memory. It features a power density of 238 $\mu$W/MHz. The Cortex-M4 core features DSP extensions which deliver high performance on data processing algorithms as well as 210 DMIPS and 566 CoreMark at 168 MHz on general purpose applications. Finally, the output of the application can be transmitted to an external device using the Bluegiga WT12 Bluetooth Class 2 Module [60].

A 6 layers Printed Circuit Board (PCB) assembles the described components in $9 \times 4.5$ cm as shown in Fig. 5, with a weight of 50 grams. The board global power supply is controlled by a dedicated integrated circuit with an internal switching voltage regulator. Each device within the board is then powered by a low-dropout (LDO) regulator[1].

Table 3: Threshold values for ST, NOM and NM. The values here exposed correspond to the threshold giving the highest accuracy values.

| Gesture | Threshold | Accuracy |
|---|---|---|
| ST | Output >1.6 | 93 |
| NM | 0.4 >= Output <1.8 | 95 |
| NOM | Output<0.3 | 97 |

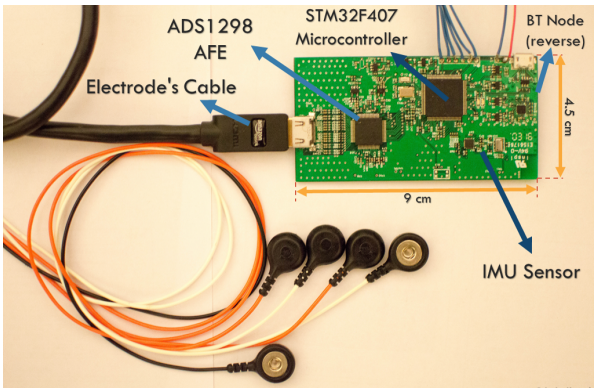


Figure 5: Assembled PCB (top) with electrodes cable. Here, two channels and the reference (GND) are wired. Only one channel (and reference) are later attached to the auto-adhesive gel-based electrodes to perform the tests.

Thanks to the compound of general purpose and power efficient devices, the resulting platform is a highly versatile system for embedded applications based on processing of bio-signals and motion. Table 4 shows the relevant features of the devices employed in the proposed system.

The algorithm, implemented on the microcontroller, rates the drowsiness level on a scale of 5 values. Once the signals have been acquired, the power spectral density (PSD) of EEG signal and the RMS of the IMU signal are calculated by exploiting the optimized Cortex microcontroller Software Interface Standard (CMSIS) DSP Software Library [61]. For the EEG part, the maximum energy value of the alpha bands is used as feature to detect drowsiness, while the RMS of the derivative of the 3-axis accelerometer of the IMU signal is used for the motion detection part. Subsection 3.4 describes the detection algorithm in details. Detected drowsiness levels can be streamed via the BT module to an Android application, developed to show the system state and the intermediate or final outputs of the processing chain.

### 3.3. Parallel Ultra Low Power Platform (PULP)

PULP[2] is a multi-core ultra low power platform exploiting near-threshold computation (NTC) and parallel

[1]The current board was developed only for testing purposes. Further optimization can reduce the size and weight of the complete hardware to a half.

[2]The first generation PULP architecture is presented in [25], while the second generation is presented in [26]. Further information regarding the PULP platform can be found in the project web page http://www.pulp-platform.org.

| | |
|---|---|
| **AFE (ADS1298)** | |
| Channels | 8 |
| Input reference Noise | 4(micro)Vpp |
| Power Consumption | 12.5 mW |
| No. of adjustable gains | 7 |
| Signal-to-noise Ratio | 112dB |
| Resolution | 24bit |
| **IMU (MPU-9150)** | |
| DOF | 9 |
| Resolution | 16bit |
| Sample Rate(Acc) | 1Khz |
| Power Consumption | 1.4mW |
| **Microcontroller (STM32F407vgt6)** | |
| Operational Frequency | 168Mhz |
| RAM | 192kB |
| Flash Memory | 1MB |
| Run mode Pw. Consumption | 152mW |
| Sleep mode Pw. Consumption | 39mW |

Table 4: Relevant features of the devices used in the system.

execution to fulfill near-sensor processing applications performance demand at a very low power budget (few mW) typical of battery-powered systems. The third embodiment of the PULP platform used in this work leverages a cluster with 4 cores which share 64kB L1 single latency tightly-coupled data memory (TCDM) to reduce the core to core communication latency, and 4kB of shared instruction cache. The processors of the cluster are based on an optimized micro-architecture implementing the OpenRISC ISA extended with power management and DSP instructions such as zero-overhead hardware loops, load and store operations with automatic pointers increment and floating-point units [62], necessary to deal with applications requiring high precision and high dynamic range. A Direct Memory Access (DMA) unit is used to explicitly transfer data from the off-cluster 256kB L2 data memory and the TCDM.

Off-cluster, several peripherals such as SPI and I2C communicate with the external word through a micro-DMA subsystem able to autonomously transfer data from the peripherals to the L2 memory while the cluster is idling, improving the energy efficiency of the system. The SoC and the cluster are in two different voltage and frequency domains to further improve energy efficiency depending on the computational workload of applications. Moreover, an automatic clock gating mechanism is used to reduce power consumption of idle resources of the system. For example, every time a core is in idle state, its clock is gated to save power. This mechanism is hidden to the programmer which uses only parallel programming primitives such as synchronization barriers implicitly embedding power management function calls. The PULP architecture has been taped-out in several technologies including UTBB FD-SOI 28nm, UMC 65nm, and GF 28nm. Fig. 6 shows the layout of the PULPv3 chip, implemented in 28nm UTBB FD-SOI technology, and used for the characterization of the performance and power models adopted in this work. The PULP platform relies on OpenMP 3.0 parallel library that operates on top of a GCC 4.9 toolchain for programming. The hardware/software environment of PULP includes a set of software tools useful to implement and debug applications that run on the architecture, and to estimate their execution time.

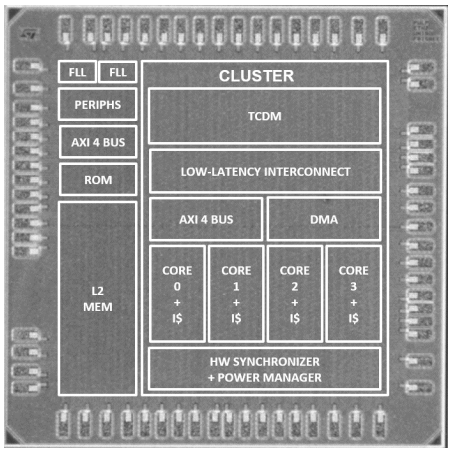


Figure 6: Layout of the PULP Chip.

To estimate the power consumption of the architecture, data have been extracted from measurements on the PULPv3 silicon prototype and adapted to the configurations actually employed in the exploration (i.e. a 4-core architecture enhanced with floating-point units).

### *3.4. Sensor Fusion Alarm system.*

The sensor fusion algorithm uses the feature extraction techniques described in section 3.1 to classify the drowsiness states. Fig. 7 shows a block diagram of the application and the description of the 5 levels of the drowsiness detection alarm are presented below.

#### *3.4.1. Level 1: Normal movement*

At the first level, only the IMU sensor is used. The system remains in this level when the blink duration is below 500ms, the user produce no alpha waves (or below threshold) and the IMU classifier reports No movement (NOM) or Normal movement (NM).

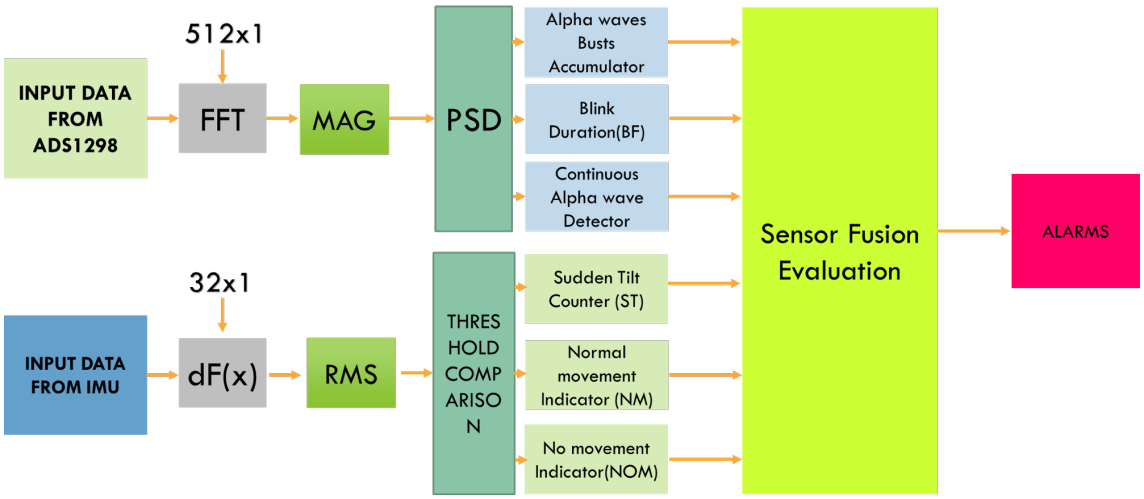


Figure 7: Block Diagram of the extracted features to compose the sensor fusion algorithm. The values are extracted/classified from the different sources using the feature extraction methods detailed in section 3.1 to serve in the identification of the different levels of alarm.

#### *3.4.2. Level 2: Blink Duration + No movement*

Two conditions are required to trigger the alarm at this level. The blink duration must be longer than 500 ms, according to previous investigations [44, 45, 46] and the gesture classification must return no movement (NM) class, used to confirm the reduced activity triggered by a drowsiness state of the user. If normal movement (NM) is reported, the value of the blink duration is set to zero, assuming that the user is not to be under drowsy conditions.

#### *3.4.3. Level 3: Alpha waves burst detection*

The occurrence of alpha waves bursts increases when the user enters in a deeper drowsiness state. Following the Objective Sleepiness Scoring (OSS) [19], it is possible to identify a drowsy state by evaluating the period on which the alpha waves level exceeds a given threshold, over a time window of 20 seconds. The alpha waves are quantified using the PSD method described before and the alarm is triggered if the value is above the threshold for at least 5 seconds on the time window.

#### *3.4.4. Level 4: Sudden tilt (nodding)*

Level 4 of drowsiness state is asserted using only the 3-axis accelerometer to recognize nodding movements of the users head, as described in section 3.1. In this alarm level, only the sudden tilt is accounted. A single event is needed to activate the alarm, since the nodding gesture represents a stronger indication of drowsiness [54, 55, 56].

#### *3.4.5. Level 5: Constant presence of alpha waves*

A constant burst of alpha waves is an indication of the closure of the eyes [47] induced by a total loss of attention or sudden sleep. Such state is detected using the same feature extraction method reported for level 3 (PSD-method). More specifically, if the maximum energy of the alpha waves stays over the threshold for more than 3 seconds, the alarm level 5 is asserted. This was considered as the highest level of alarm since it corresponds to the most dangerous situation where the user is falling asleep.

### *3.5. Implementation on the PULP architecture.*

This section describes the implementation of the 5-levels drowsiness detection alarm system on a 4-cores PULP architecture. The PULP software toolchain has been used to evaluate the parameters of the system simulating the architectural configurations not necessarily implemented on the silicon prototypes, such as floating-point units. The ANSI C code used for the implementation on the MCU has been parallelized using the OpenMP 3.0 parallel programming interface and optimized for the PULP architecture.

Since the most compute demanding part of the algorithm is the FFT, a great effort has been spent to optimize this kernel on the PULP architecture, exploiting a fine-grained data-parallel scheme supported by the programming model. The FFT algorithm requires to compute a set of butterflies on the N input samples (where N is the size of FFT, 512 for this application) for each stage of computation, and the number of stages is equal to the 2-base logarithm of the number of input samples

(9 in this case). In the baseline radix-2 algorithm, after each stage, data generated by the butterflies of the previous stage has to be shuffled to compute the butterflies on the following stage.

On the PULP architecture, the FFT is computed by splitting the butterflies calculation homogeneously among the four cores, and synchronizing the cores using hardware barriers after each stage of butterflies to maintain the data consistency. Two different implementations have been evaluated, described in the following.

As explained above, the baseline radix-2 FFT requires a synchronization barrier after each stage of butterflies (i.e. 9 barriers), leading to a relevant synchronization overhead not amortized by the small computational load required by each stage of butterflies. A more optimized approach relies on the radix-8 algorithm. Exploiting this implementation, each butterfly performs a single Discrete Fourier Transform (DFT) among 8 samples instead of 2 as in the case of the radix-2 implementation. This reduces the number of butterflies to be computed at each stage but it increases the computational complexity of each butterfly. The proposed implementation is composed of 3 stages each with 64 butterflies (16 for each core), therefore 3 barriers are triggered to accomplish the full 512 samples FFT. Hence, this approach increases the available parallelism and reduces the synchronization overhead with respect to the radix-2 algorithm. The computation of the magnitude of the FFT is parallelized by dividing the signal by 4, thus each core works independently without synchronizations. Both the FFT and magnitude parallel implementations feature a speedup greater than 3.9 w.r.t. the single core version on PULP, showing a quasi-ideal parallel speedup in performance.

Regarding the computation part related to the IMU signal, the RMS envelope is computed on the last 512 samples instead to 32 since it offers more efficient use of cores. A parallel version was implemented by splitting again the signal in four parts. Each core computes the summation of the square of the signal assigned and finally the cores are synchronized. In the last phase, a single core is in charge to sum the four results and to compute the square root.

## 4. Experimental Results

### *4.1. Experimental setup*

Testing a drowsiness detection system is not a trivial task. Using a real scenario, where a drowsy person drives a car, exposes the test subject to dangerous situations, hence it is not feasible. On the other hand, while simulators offer a realistic perception of the driving experience in a safe environment, it is proven that the reactions of the driver in a simulated scenario and on a real car are different [65, 66]. Differences are mostly caused by the awareness of being in a safe environment. For these reasons, the test of the proposed system is performed on simulated events, with a combination of behavioural and physiological symptoms of the drowsiness. This approach has already been validated by previous works, and demonstrated to be an effective and reliable way to test drowsiness detection [67, 66, 68, 69].

The 5-level alarm system described in section 3.2 is tested on 10 healthy subjects with no previous history of neural diseases. The participants were under sleep deprivation (3 hours of sleep) the day before the test. Additionally, to maximize the drowsiness effects, the tests were conducted at late night hours. The evaluation was performed in real-time using the hardware-software implementation presented in section 3. The board is placed on the subject's head, as shown in Fig. 1. The electrodes are located at Oz (Positive electrode) and Fpz (Negative electrode), following the 10-20 reference system [70], while the reference electrode is placed behind the ear. Subjects reported that the device did not cause appreciable discomfort (after approx. 30 min. of testing, for each test subject).

To test the first level, the test subjects were asked to move normally. The second level was tested by asking to increase the blink duration while avoiding any rough movement. For the third level, the test subjects were asked to close their eyes for short periods of time (<500ms) to generate bursts of alpha waves, easily detectable because of the induced drowsy conditions. For the fourth level, nodding gesture were simulated. For the last level, the test subjects were asked to close their eyes completely. Each level was tested for a maximum time frame of 1 minute.

### *4.2. Test evaluation*

All the classification results computed on the embedded platform are can be visualized through an Android application. During the test, each alarm level is assessed separately, leading to a binary evaluation of each level (fail/pass). Each test subject simulates the alarm conditions 5 times. The accuracy values are finally obtained after extracting the percentage of fail/pass events for each alarm. The pass/fail condition depends on the performed test. The first level is identified as fail if any alarm is triggered over 1 minute of normal activity performed by the subject. The second level fails if the alarm is not triggered after closing the eyes for

Table 5: Comparison with SoA systems for drowsiness detection.

| Author | Method | Advantage | Disadvantage | Accuracy | Platform | Intrusive |
|---|---|---|---|---|---|---|
| [63] | EEG, Neural Network | Single EEG Channel | Training, Offline | 83 | Computer | - |
| [64] | Cam, Eye parameters | real-time | Fixed, not wearable, Comp. Hungry | 94 | NS | NO |
| [43] | NIRS, EEG, Alpha Pw | Portable | Noise, Redundant Measurements | 65-88 | MCU | NO |
| [10] | EEG ($\alpha$&$\delta Pw$), IMU (Gesture) | Helmet based, dry electrodes, no training | No dedicated ADC, mainly based on IMU, E.Eff. not mentioned, Lp. MCU | NS | MCU | NO |
| This work | EEG (Blink Dur. $\alpha Pw$), IMU (Gesture) | Mult. features, Reduced. HW, No training, wearable | Noise, Gel-based electrodes | 88-100 | MCU | NO |

more than 500ms while performing no movement. Regarding the third level, the test fails if the alarm is not triggered after the corresponding evaluation window (20 seconds). In the case of the fourth level, the detection must be done on a single nodding event. For the last level, the detection fails if the system does not detect the condition after 3 seconds from the closure of the eyes.

Fig. 8 shows the experimental results, where average accuracy reaches to 95.2% over 250 samples. It is noteworthy that the lowest accuracy is measured in pure alpha wave detection, confirming the high variability of purely physiological detection and the added value of a sensor fusion approach to improve the robustness of detection.

### 4.3. Embedded system performance

Fig. 9 shows the system power consumption with the contributions from the ADC, IMU, the microcontroller and the BT radio. In this implementation, the MCU operates at 168 MHz when receiving a new sample or executing the processing algorithm.

Since the ADC and the IMU notify the acquisition of a new sample using interruptions, the microcontroller can be put in sleep mode while waiting for a new sample, significantly reducing the average power consumption (power consumption of run mode is 383% higher than sleep mode[3]). This operation does not affect the real-time behavior since the system wakes up every 2ms to buffer EEG data or to compute the alarm when the corresponding buffer is full, as shown in Fig. 10. The sampling of IMU data is much less critical since a new data is available every 20ms.

We notice that during the active state the digital processing dominates the power consumption of the system, since the microcontroller calculates the RMS and the FFT on partially overlapped windows of IMU and EEG data with a stride of 10 and 32 samples respectively. The PSD calculation is the most demanding part of the digital processing since it uses 60k cycles while the RMS requires less than 3k cycles.

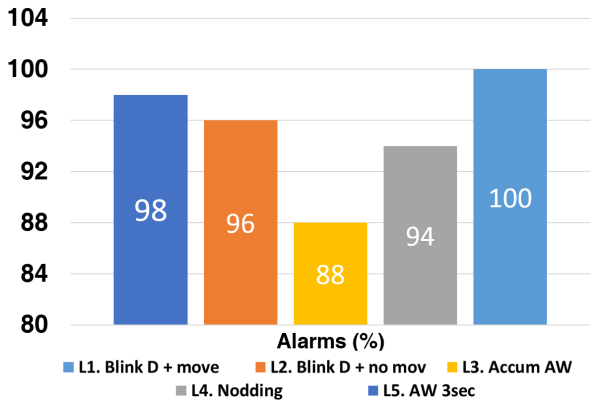


Figure 8: Detection accuracy of the different alarms. Following the criteria described in section 4.2, the accuracy values are obtained after extracting the percentage of fail/pass events for each alarm.

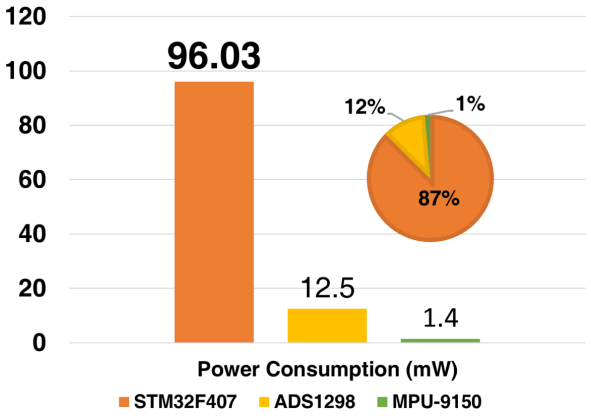


Figure 9: Power consumption of the embedded implementation (on PCB). The MCU dominates the power consumption, employing 87% of the total power.

### 4.4. Comparison with state-of-art systems

Table 5 presents a comparison between the proposed system and other State of Art (SoA) approaches.

[3]The value has been calculated after measuring the current consumption of the chip in both operational modes. The obtained values are similar to the product specification of the STM32F407 [71].

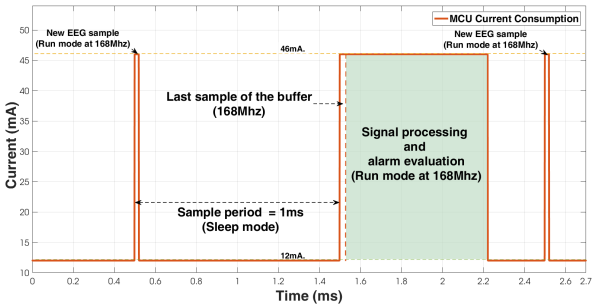


Figure 10: The EEG and IMU samples are collected using interruptions. The processor wakes up at run mode (168Mhz) when a new sample arrives. During the waiting period, the MCU remains at sleep mode, reducing the global power consumption. When the EEG/IMU buffers are full (every 64 samples for the EEG buffer and every 32 samples for the IMU buffer) the MCU performs the required signal processing and transmits the corresponding alarm levels to a smartphone running the Android application. The figure above shows the duty-cycle of the microcontroller for the EEG acquisition. The same applies for the IMU samples at the corresponding sample rate (50 Hz).

In [63] the algorithm for drowsiness detection runs on a PC and the computational complexity of this approach rules out the possibility of a low power embedded implementation. The work presented in [43] describes a low power device capable to operate for 6 hours with a 200mAh battery. The system fuses EEG signals and NIRs classification to measure only brain activity not exploiting other behavioral or physiological features. Our implementation, thanks to the fusion of behavioral and physiological features from the two sensors, obtains a better accuracy and increases the rate of detection by considering more drowsiness-related events with fully portable hardware, achieving 20% more energy efficiency.

In [10] a sensor fusion system exploiting EEG signals in conjunction with IMU-based user motion tracking is introduced. However, the presented work mainly leverages the IMU sensor for the detection of the drowsiness levels, not providing insights about the usage of the EEG signal. Furthermore, accuracy estimates and energy efficiency of the system are not provided, preventing a direct comparison.

The main drawback of the system proposed in this paper consists of the usage of gel-based electrodes, which somehow limits its flexibility. However, as opposed to passive dry electrodes, current SoA active dry electrodes achieve very comparable performance with respect to wet electrodes [72] and they are more suitable for wearable deployments. Nevertheless, the adoption of dry or in-ear active electrodes will be subject of future work since it is essential for real-life applications.

Our MCU-based implementation leverages the use of multi-feature analysis from both the EEG and IMU sensors and it provides a wearable system with a battery duration of at least 6 hours and an accuracy of 95.2% while significantly shortening the delay in taking countermeasures, hence reducing the probability of accidents happening in the period between the onset of drowsiness condition and its detection.

### *4.5. Implementation on PULP*

To evaluate the performance and energy consumption of the computing platforms adopted in the system (i.e., PULP and CortexM4-based MCUs), only the compute-intensive kernels, responsible for more than 99% of the overall computational load of the algorithm have been analyzed. Table 6 shows the the number of cycles needed to perform the FFT, Magnitude and RMS functions in both platforms, as well as a comparison of the execution time of the different solutions. While the code running on the CortexM4 architecture relies on heavily optimized CMSIS libraries, the implementation on PULP is based on an ANSI C implementation of the algorithms with OpenMP extensions for parallelization.

Nevertheless, although the ARM Cortex M4 core performs slightly better with respect to the single-core PULP architecture for some of the kernels, a single core PULP platform provide an almost 20% speed-up with respect to the CortexM4 for the Magnitude function, while relying on a fully flexible C implementation of the algorithm. The situation dramatically changes when executing the algorithms exploiting parallel processing over the 4 cores of the PULP platform. In this case the execution time with respect to the CortexM4 processor reduces by up to 4.66x. It can be noted that for the kernels with high parallelism, like FFT and Magnitude, that account for more than 95% of the overall computational load during sequential execution, the speed-up is nearly ideal. The only function not easily parallelizable is the RMS 32s, due to a small dataset, and hence parallelism, but it has a negligible impact on the overall execution time of the application.

An important factor to take into consideration for the calculation of the energy efficiency is the minimum latency required to achieve the real-time constraint. Indeed, to avoid sample loss, all the signal processing must be finished in a time no longer than 2ms. This constraint was taken into account to adjust the clock frequency of the PULP platform with the goal of comparing the execution with minimal energy consumption. Table 7 shows the real-time frequency of the analyzed computing platforms, which includes one high-end MCU STM32F407x and one ultra-low-power MCU

Table 6: Number of cycles required to compute each function in the analyzed embedded computing platforms [KCycles]. The FFT calculation is the most computationally demanding operation. Given its highly parallelizable computational algorithm, the 4-core PULP MCU reaches nearly ideal speedup.

| Kernel Func | Single Core ARM CMSIS | Pulp 1 Core | Pulp 4 Cores | ARM/SCPulp | ARM/4CPulp | SCPulp/4CPulp |
|---|---|---|---|---|---|---|
| **FFT RADIX8** | 42.90 | 64.03 | 16.69 | 0.67 | 2.57 | 3.84 |
| **Magnitude** | 17.87 | 15.17 | 3.83 | 1.18 | 4.66 | 3.96 |
| **RMS (32s)** | 0.26 | 0.30 | 0.16 | 0.86 | 1.67 | 1.94 |
| **RMS(512s)** | 2.52 | 2.95 | 0.83 | 0.86 | 3.05 | 3.56 |

Ambiq Apollo, both based on CortexM4 processor, and PULP executing on a single core and on 4 cores. In Fig. 11 we see that this task cannot be accomplished by a low-power MCU like Ambiq Apollo, due to its limited maximum operating frequency (24 MHz).

On PULP, the frequency required to maintain the latency obviously decreases when increasing the number of cores. This, coupled with the near-threshold computing capabilities of the PULP platform aim towards a significant improvement in energy efficiency. This concept is well highlighted in Fig. 12, which also shows the comparison with off-the-shelf MCUs that operates at nominal voltage supply of 1.8V and 2.5V. The difference in energy between the MCUs and the single-core PULP platform at the nominal supply voltage is mainly given by technology gap, different implementation strategy and architectural complexity, which leads to 8.6x to 45.2x lower energy consumption.

More interesting is the exploitation of parallel near threshold computing on the PULP platform, leading to a further improvement of 3.4x in performance with respect to sequential processing, and to an improvement of 12.1x and 63.3x in terms of energy consumption with respect to commercial MCUs.

From an application perspective, these results show that the optimization of the parallel processing tailored for a highly efficient HW/SW platform allows to extend the battery life of the whole system to 46 hours, leading to an improvement of 7 times with respect to a solution based on a commercial MCU.

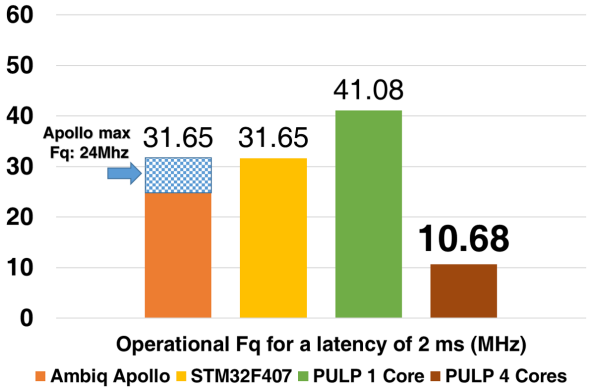


Figure 11: Minimal operating frequency required to achieve real-time operation. Featuring parallelization, the 4-cores PULP implementation is capable to work at a considerable lower frequency than the other cores, favoring voltage scaling and hence energy saving.

Table 7: Comparison between different platforms. The real-time frequency (RT freq) corresponds to the frequency required to achieve real-time operation. This is an important factor regarding energy consumption together with the operating voltage (Vdd). Ambiq Apollo features a lower power consumption but it does not achieve the required frequencies (i.e. max frequency is 24 MHz). The 4-cores PULP MCU delivers best energy efficiency while meeting the real-time constraint of the application.

| MCU | A. Apollo | STM32F407 | 1C PULP | 4C PULP |
|---|---|---|---|---|
| **No. of Cores** | 1 | 1 | 1 | 4 |
| **RT Freq [MHz]** | 31.68 | 31.68 | 45.59 | 11.76 |
| **Vdd (V)** | 1.80 | 2.50 | 0.48 | 0.45 |
| **Pw Dens [µW/MHz]** | 115 | 600 | 10.27 | 27.64 |
| **Power [mW]** | 3.64 | 18.99 | 0.42 | 0.30 |
| **Energy[µJ]** | 7.28 | 37.97 | 0.84 | 0.59 |

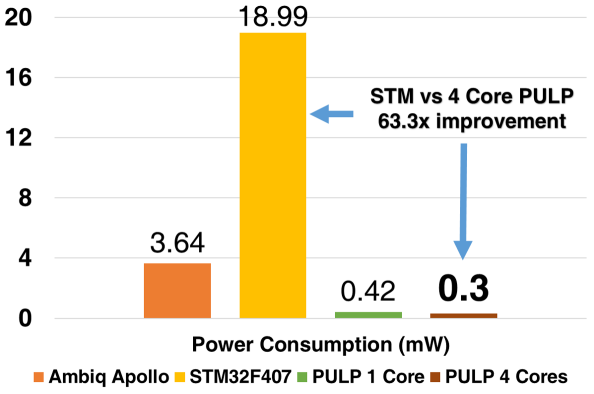


Figure 12: Power consumption comparison between different platforms. The 4-cores PULP MCU offers 63x energy saving with respect to the implementation on STM32F407.

## 5. Conclusion

Drowsiness is one of the root causes of accidents in many industrial and transportation environments, since high levels of fatigue affect attention and impair drivers and operators abilities. The drowsiness detection is a challenge because the clinical parameters to quantify the drowsiness are not clearly defined and the systems to detect drowsiness and fatigue level should target unobtrusiveness and energy efficiency. This work introduces a drowsiness detection system based on sensor fusion techniques implemented on a low power embedded processor. Many of the current implementations scan a single parameter, while fatigue and drowsiness symptoms are highly variable among the population. Using physiological and behavioral indicators, we present an embedded solution with 5 levels of drowsiness detection, obtained combining a single channel EEG signal and user motion collected form an IMU.

The accuracy detection of our system reaches with 95.2%, on 10 test subjects. Thanks to the power management done on the board, the system reaches 6 hours of life with a 200mAh Li-Ion battery, when the algorithm is implemented on a commercial MCU. Furthermore, we implemented the drowsiness detection algorithm on a parallel ultra low power platform providing a boost in energy efficiency by 63x with respect to the commercial MCU. At system level, this approach extends the battery life by 7x paving the way for a fully wearable always-on solution with a battery-life of 46 hours.

Future work will target further optimization of the algorithm on the PULP platform, the optimization of the EEG sensor interface introducing non-intrusive dry active electrodes, such as in-ear electrodes [73], the miniaturization of the current device and the test of the system on a larger number of subjects to improve the robustness of the detection. We will also explore feature extraction techniques for other EEG bands considering that alpha waves are not present in 10% of the world population [1, 20].

## Acknowledgments

This work was funded by the Swiss National Science Foundation under grant 162524 (MicroLearn: Micropower Deep Learning), armasuisse Science & Technology, by the ERC MultiTherman project (ERC-AdG-291125), and by the OPRECOMP project founded from the European Unions Horizon 2020 research and innovation programme under grant agreement No 732631.

## References

[1] T. K. Aich, Absent posterior alpha rhythm: An indirect indicator of seizure disorder?, Indian journal of psychiatry 56 (1) (2014) 61.

[2] D. Dinges, M. M. Mallis, G. Maislin, J. W. Powell IV, Evaluation of techniques for ocularmeasurement as an index of fatigue andthe basis for alertness management, in: National Highway Traffic Safety Administration, 1998, p. 113.

[3] Q. Ji, Z. Zhu, P. Lan, Real-time nonintrusive monitoring and prediction of driver fatigue, IEEE transactions on vehicular technology 53 (4) (2004) 1052–1068.

[4] F. C. D. G. e. a. T. Akerstedt, C. Bassetti, Sleepiness at the wheel, white paper, in: Sleepiness at the Wheel, White Paper, Institut National Du Sommeil et de la Vigilance, 2013.

[5] H. Cai, Y. Lin, A roadside its data bus prototype for intelligent highways, IEEE Transactions on intelligent transportation systems 9 (2) (2008) 344–348.

[6] MOBILEYE, `http://www.mobileye.com/technology/applications/lane-detection/` (2016).

[7] Mercedes-Benz, `https://www.mbusa.com/mercedes/technology/videos/detail/title-safety/videoId-710835ab8d127410VgnVCM100000ccec1e35RCRD` (2016).

[8] D. Sommer, M. Golz, Evaluation of perclos based current fatigue monitoring technologies, in: 2010 Annual International Conference of the IEEE Engineering in Medicine and Biology, 2010, pp. 4456–4459. doi:10.1109/IEMBS.2010.5625960.

[9] A. Samuel, A. Lawoyin, A novel application of inertial measurement units (imus) as vehicular technologies for drowsy driving detection via steering wheel movement, Open Journal of Safety Science and Technology 4.

[10] P. Li, R. Meziane, M. J. D. Otis, H. Ezzaidi, P. Cardou, A smart safety helmet using imu and eeg sensors for worker fatigue detection, in: 2014 IEEE International Symposium on Robotic and Sensors Environments (ROSE) Proceedings, 2014, pp. 55–60.

[11] F. Li, X. Wang, Eye indicators and driving fatigue research based on driving simulator, in: CICTP 2014: Safe, Smart, and Sustainable Multimodal Transportation Systems, ASCE, 2014, pp. 2463–2471.

[12] A. Kokonozi, E. Michail, I. Chouvarda, N. Maglaveras, A study of heart rate and brain system complexity and their interaction in sleep-deprived subjects, in: 2008 Computers in Cardiology, IEEE, 2008, pp. 969–971.

[13] R. N. Khushaba, S. Kodagoda, S. Lal, G. Dissanayake, Driver drowsiness classification using fuzzy wavelet-packet-based feature-extraction algorithm, IEEE Transactions on Biomedical Engineering 58 (1) (2011) 121–131. doi:10.1109/TBME.2010.2077291.

[14] G. Yang, Y. Lin, P. Bhattacharya, A driver fatigue recognition model based on information fusion and dynamic bayesian network, Information Sciences 180 (10) (2010) 1942–1954.

[15] H. Ueno, M. Kaneda, M. Tsukino, Development of drowsiness detection system, in: Vehicle Navigation and Information Systems Conference, 1994. Proceedings., 1994, IEEE, 1994, pp. 15–20.

[16] H. S. Shin, S. J. Jung, J. J. Kim, W. Y. Chung, Real time car driver's condition monitoring system, in: 2010 IEEE Sensors, 2010, pp. 951–954.

[17] H. V. Huikuri, A. Ylitalo, S. M. Pikkujämsä, M. J. Ikäheimo, K. J. Airaksinen, A. O. Rantala, M. Lilja, Y. A. Kesäniemi, Heart rate variability in systemic hypertension, The American journal of cardiology 77 (12) (1996) 1073–1077.

[18] B. H. Friedman, J. F. Thayer, Autonomic balance revisited:

panic anxiety and heart rate variability, Journal of psychosomatic research 44 (1) (1998) 133–151.

[19] A. Muzet, T. Pébayle, J. Langrognet, S. Otmani, Awake pilot study no. 2: Testing steering grip sensor measures, CEPA, Gatineau, QC, Canada, Tech. Rep. IST-2000-28062.

[20] F. PLUM, Handbook of electroencephalography and clinical neurophysiology, Archives of Neurology 26 (6) (1972) 556–556.

[21] M. Akin, M. B. Kurt, N. Sezgin, M. Bayram, Estimating vigilance level by using eeg and emg signals, Neural Computing and Applications 17 (3) (2008) 227–236.

[22] U. H. et al., A multimodal drowsiness monitoring ear-module system with closed-loop real-time alarm, in: IEEE International Conference on Biomedical circuits and Systems (BIOCAS) Proceedings, IEEE, 2016.

[23] U. H. et al., An eeg-nirs ear-module soc for wearable drowsiness monitoring system, in: IEEE Asian solid state circuit conference (ASSCC) Proceedings, Vol. 9, IEEE, 2016, pp. 344–348.

[24] S. Benatti, B. Milosevic, M. Tomasini, E. Farella, P. Schonle, P. Bunjaku, G. Rovere, S. Fateh, Q. Huang, L. Benini, Multiple biopotentials acquisition system for wearable applications, in: International Conference on Biomedical Electronics and Devices (BIODEVICES), Scitepress, 2015, pp. 260–268.

[25] D. Rossi, A. Pullini, I. Loi, M. Gautschi, F. K. Grkaynak, A. Bartolini, P. Flatresse, L. Benini, A 60 gops/w, -1.8 v to 0.9 v body bias ulp cluster in 28nm utbb fd-soi technology, Solid-State Electronics 117 (2016) 170 – 184, {PLANAR} FULLY-DEPLETED {SOI} {TECHNOLOGY}. doi:http://dx.doi.org/10.1016/j.sse.2015.11.015.
URL http://www.sciencedirect.com/science/article/pii/S0038110115003342

[26] D. Rossi, A. Pullini, I. Loi, M. Gautschi, F. K. Gurkaynak, A. Teman, J. Constantin, A. Burg, I. Miro-Panades, E. Beign, F. Clermidy, F. Abouzeid, P. Flatresse, L. Benini, 193 mops/mw @ 162 mops, 0.32v to 1.15v voltage range multi-core accelerator for energy efficient parallel and sequential digital processing, in: 2016 IEEE Symposium in Low-Power and High-Speed Chips (COOL CHIPS XIX), 2016, pp. 1–3. doi:10.1109/CoolChips.2016.7503670.

[27] C. Xu, X. Wang, X. Chen, Modeling Fatigue Level by Driver's Lane-Keeping Indicators, pp. 2282–2288. arXiv:http://ascelibrary.org/doi/pdf/10.1061/9780784413159.331, doi:10.1061/9780784413159.331.
URL http://ascelibrary.org/doi/abs/10.1061/9780784413159.331

[28] J. Krajewski, D. Sommer, M. Golz, U. Trutschel, D. J. Edwards, Steering wheel behavior based estimation of fatigue, in: Proceedings of the 5th International Driving Symposium on Human Factors in Driver Assessment and Design, 2009, pp. 118–124.

[29] M. Flores, J. Armingol, A. de la Escalera, Driver drowsiness warning system using visual information for both diurnal and nocturnal illumination conditions, EURASIP Journal on Advances in Signal Processing 2010 (1) (2010) 438205. doi:10.1155/2010/438205.
URL http://dx.doi.org/10.1155/2010/438205

[30] Q. Ji, Z. Zhu, P. Lan, Real-time nonintrusive monitoring and prediction of driver fatigue, IEEE Transactions on Vehicular Technology 53 (4) (2004) 1052–1068. doi:10.1109/TVT.2004.830974.

[31] A. Kolli, A. Fasih, F. A. Machot, K. Kyamakya, Non-intrusive car driver's emotion recognition using thermal camera, in: Proceedings of the Joint INDS'11 ISTET'11, 2011, pp. 1–5. doi:10.1109/INDS.2011.6024802.

[32] G. Fortino, R. Giannantonio, R. Gravina, P. Kuryloski, R. Jafari, Enabling effective programming and flexible management of efficient body sensor network applications, IEEE Transactions on Human-Machine Systems 43 (1) (2013) 115–133.

[33] R. Gravina, P. Alinia, H. Ghasemzadeh, G. Fortino, Multi-sensor fusion in body sensor networks: State-of-the-art and research challenges, Information Fusion 35 (2017) 68 – 80. doi:http://dx.doi.org/10.1016/j.inffus.2016.09.005.
URL http://www.sciencedirect.com/science/article/pii/S156625351630077X

[34] B. Khaleghi, A. Khamis, F. O. Karray, S. N. Razavi, Multisensor data fusion: A review of the state-of-the-art, Information Fusion 14 (1) (2013) 28 – 44. doi:http://dx.doi.org/10.1016/j.inffus.2011.08.001.
URL http://www.sciencedirect.com/science/article/pii/S1566253511000558

[35] G. Fortino, S. Galzarano, R. Gravina, W. Li, A framework for collaborative computing and multi-sensor data fusion in body sensor networks, Information Fusion 22 (2015) 50 – 70. doi:http://dx.doi.org/10.1016/j.inffus.2014.03.005.
URL http://www.sciencedirect.com/science/article/pii/S156625351400044X

[36] A. Sathyanarayana, P. Boyraz, J. H. Hansen, Information fusion for robust ¢context and driver aware¢¢ active vehicle safety systems, Information Fusion 12 (4) (2011) 293 – 303, special Issue on Information Fusion for Cognitive Automobiles. doi:http://dx.doi.org/10.1016/j.inffus.2010.06.004.
URL http://www.sciencedirect.com/science/article/pii/S1566253510000679

[37] B.-G. Lee, W.-Y. Chung, A smartphone-based driver safety monitoring system using data fusion, Sensors 12 (12) (2012) 17536. doi:10.3390/s121217536.
URL http://www.mdpi.com/1424-8220/12/12/17536

[38] A. Reyes-Muoz, M. C. Domingo, M. A. Lpez-Trinidad, J. L. Delgado, Integration of body sensor networks and vehicular ad-hoc networks for traffic safety, Sensors 16 (1) (2016) 107. doi:10.3390/s16010107.
URL http://www.mdpi.com/1424-8220/16/1/107

[39] Y. Sun, X. Yu, An innovative nonintrusive driver assistance system for vital signal monitoring, IEEE Journal of Biomedical and Health Informatics 18 (6) (2014) 1932–1939. doi:10.1109/JBHI.2014.2305403.

[40] C.-T. Lin, R.-C. Wu, S.-F. Liang, W.-H. Chao, Y.-J. Chen, T.-P. Jung, Eeg-based drowsiness estimation for safety driving using independent component analysis, IEEE Transactions on Circuits and Systems I: Regular Papers 52 (12) (2005) 2726–2738.

[41] S. Hu, G. Zheng, Driver drowsiness detection with eyelid related parameters by support vector machine, Expert Systems with Applications 36 (4) (2009) 7651 – 7658. doi:http://dx.doi.org/10.1016/j.eswa.2008.09.030.
URL http://www.sciencedirect.com/science/article/pii/S0957417408006714

[42] C. T. Lin, C. J. Chang, B. S. Lin, S. H. Hung, C. F. Chao, I. J. Wang, A real-time wireless brain x2013;computer interface system for drowsiness detection, IEEE Transactions on Biomedical Circuits and Systems 4 (4) (2010) 214–222.

[43] U. Ha, H.-J. Yoo, A multimodal drowsiness monitoring ear-module system with closed-loop real-time alarm, in: IEEE Biomedical Circuits and Systems Conference (BioCAS), 2016.

[44] G. Borghini, L. Astolfi, G. Vecchiato, D. Mattia, F. Babiloni, Measuring neurophysiological signals in aircraft pilots and car drivers for the assessment of mental workload, fatigue and drowsiness, Neuroscience Biobehavioral Reviews 44 (2014) 58 – 75, applied Neuroscience: Models, methods, theories, reviews. A Society of Applied Neuroscience (SAN) special issue. doi:http://dx.doi.org/10.1016/j.neubiorev.2012.10.003.
URL http://www.sciencedirect.com/science/

article/pii/S0149763412001704
[45] R. Schleicher, N. Galley, S. Briest, L. Galley, Blinks and saccades as indicators of fatigue in sleepiness warnings: looking tired?, Ergonomics 51 (7) (2008) 982–1010.
[46] M. Johns, et al., The amplitude-velocity ratio of blinks: a new method for monitoring drowsiness, Sleep 26 (2003) A51.
[47] I. William O. Tatum, Handbook of EEG Interpretation, Second Edition, Springer Publishing Company, 2014.
URL https://books.google.it/books?id=PZnSCgAAQBAJ
[48] E. Niedermeyer, F. L. da Silva, Electroencephalography: basic principles, clinical applications, and related fields, Lippincott Williams & Wilkins, 2005.
[49] A. Anund, et al., Pilot 15report: Vti, Swedish National Road and Transport Research Institute.
[50] A. Picot, et al., On-line automatic detection of driver drowsiness using a single electroencephalographic channel, in: EMBC, 2008.
[51] J. Park, et al., Wireless dry eeg for drowsiness detection, in: EMBC, 2011, pp. 3298–3301.
[52] J. Wu, J. Cheng, et al., Bayesian co-boosting for multi-modal gesture recognition., Journal of Machine Learning Research 15 (1) (2014) 3013–3036.
[53] A. Y. Benbasat, J. A. Paradiso, An Inertial Measurement Framework for Gesture Recognition and Applications, 2002.
[54] W. Vanlaar, H. Simpson, D. Mayhew, R. Robertson, Fatigued and drowsy driving: A survey of attitudes, opinions and behaviors, Journal of Safety Research 39 (3) (2008) 303 – 309. doi:http://dx.doi.org/10.1016/j.jsr.2007.12.007.
URL http://www.sciencedirect.com/science/article/pii/S0022437508000492
[55] A. Heitmann, R. Guttkuhn, A. Aguirre, U. Trutschel, M. Moore-Ede, Technologies for the monitoring and prevention of driver fatigue, in: Proceedings of the first international driving symposium on human factors in driver assessment, training and vehicle design, Vol. 86, 2001.
[56] M. hoseyn Sigari, M. reza Pourshahabi, M. Soryani, M. Fathy, A review on driver face monitoring systems for fatigue and distraction detection.
[57] Texas Instruments, http://www.ti.com/lit/ds/symlink/ads1298.pdf (2015).
[58] invensense, https://www.invensense.com/wp-content/uploads/2015/02/MPU-9150-Datasheet.pdf (2013).
[59] STMicroelectronics, http://www.st.com/en/microcontrollers/stm32f407vg.html (2016).
[60] Silicon Labs, https://www.silabs.com/products/wireless/bluetooth/bluetooth-classic-modules/Pages/wt12-bluetooth-class-2-module.aspx (2016).
[61] ARM, https://www.arm.com/products/processors/cortex-m/cortex-microcontroller-software-interface-standard.php (2016).
[62] M. Gautschi, M. Schaffner, F. K. Grkaynak, L. Benini, 4.6 a 65nm cmos 6.4-to-29.2pj/flop@0.8v shared logarithmic floating point unit for acceleration of nonlinear function kernels in a tightly coupled processor cluster, in: 2016 IEEE International Solid-State Circuits Conference (ISSCC), 2016, pp. 82–83. doi:10.1109/ISSCC.2016.7417917.
[63] A. G. Correa, et al., Automatic detection of drowsiness in {EEG} records based on multimodal analysis, Medical Engineering Physics.
[64] A. Rahman, et al., Real time drowsiness detection using eye blink monitoring, in: NSEC, IEEE, 2015, pp. 1–7.
[65] F. Bella, Driver perception of roadside configurations on two-lane rural roads: Effects on speed and lateral placement, Accident Analysis & Prevention 50 (2013) 251–262.
[66] A. Sahayadhas, et al., Detecting driver drowsiness based on sensors: a review, Sensors 12 (12) (2012) 16937–16953.
[67] M. E. Howard, M. L. Jackson, D. Berlowitz, F. ODonoghue, P. Swann, J. Westlake, V. Wilkinson, R. J. Pierce, Specific sleepiness symptoms are indicators of performance impairment during sleep deprivation, Accident Analysis Prevention 62 (2014) 1 – 8. doi:http://dx.doi.org/10.1016/j.aap.2013.09.003.
URL http://www.sciencedirect.com/science/article/pii/S0001457513003564
[68] Q. Ji, X. Yang, Real-time eye, gaze, and face pose tracking for monitoring driver vigilance, Real-Time Imaging 8 (5) (2002) 357 – 377. doi:http://dx.doi.org/10.1006/rtim.2002.0279.
URL http://www.sciencedirect.com/science/article/pii/S1077201402902792
[69] A. Rahman, et al., Real time drowsiness detection using eye blink monitoring, in: NSEC, IEEE, 2015, pp. 1–7.
[70] V. Jurcak, D. Tsuzuki, I. Dan, 10/20, 10/10, and 10/5 systems revisited: their validity as relative head-surface-based positioning systems, Neuroimage 34 (4) (2007) 1600–1611.
[71] STM, STM32F405/415, STM32F407/417, STM32F427/437 and STM32F429/439 advanced ARM-based 32-bit MCUs, rev. 15 (7 2017).
[72] J. Xu, R. F. Yazicioglu, B. Grundlehner, P. Harpe, K. A. A. Makinwa, C. V. Hoof, A 160uw 8-channel active electrode system for eeg monitoring, IEEE Transactions on Biomedical Circuits and Systems 5 (6) (2011) 555–567.
[73] D. Looney, V. Goverdovsky, I. Rosenzweig, M. J. Morrell, D. P. Mandic, Wearable in-ear encephalography sensor for monitoring sleep. preliminary observations from nap studies, Annals of the American Thoracic Society 13 (12) (2016) 2229–2233.